

# ELM Milestone Progress Report

## Second Quarter FY06

### March 31, 2006

A. Bayliss, D. Brennan, S. Kruger, A. Pankin, D. Schnack,  
C. Sovinec, H. Strauss with support from the NIMROD and M3D teams.<sup>1</sup>

#### Executive Summary

In this report we present the successful completion of the 2006 Q2 milestone. The statement of the milestone is as follows: *Q2 (March 31, 2006): Perform extended, linear perturbation studies to investigate the role of plasma edge density gradients. The density profiles will be used in spatially varying diffusivity coefficients, and they will be incorporated in extended-MHD effects. The shaping of the computational domain will also be improved to more accurately represent the DIII-D wall.* Studies are presented utilizing both the NIMROD and M3D codes with a range of density profiles and with improved representation of the boundary for both DIII-D and ITER geometries. In addition, the 2-fluid model in NIMROD has passed an important benchmark, and experience was gained in running simulation studies with over 40 toroidal modes. This experience will contribute to the successful completion of the remaining 2006 milestones.

#### Section I: Studies with the NIMROD Code:

##### 1.1 DIII-D Equilibria

Several equilibria based on DIII-D experimental shots *113207* and *113317* have been produced. Shot *113207* has higher density, pressure, and magnetic field than shot *113317*. A comparison of the pressure and density profiles for the two shots is shown in Figures 1a,b. A cross-section of the equilibrium for shot *113317* is shown in Figure 2.

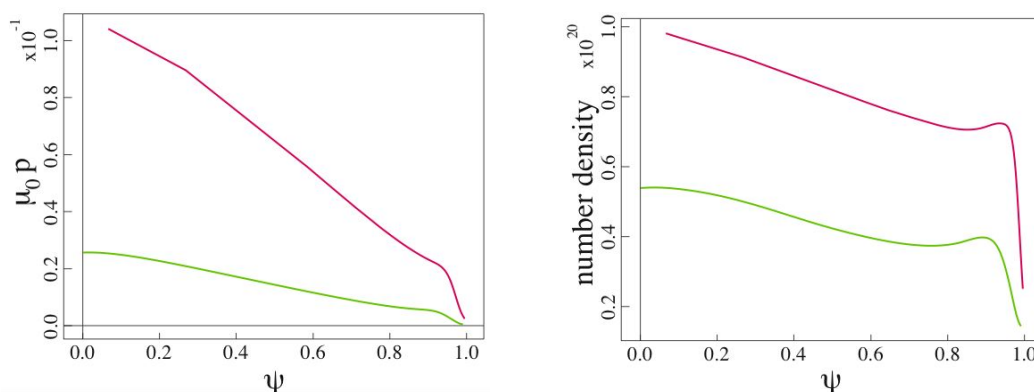


**Figure 1** (a) Equilibrium pressure profiles for reconstructions of DIII-D shots 113207 (red) and 113317 (green). **1(b)** Equilibrium density profiles for reconstructions of DIII-D shots 113207 (red) and 113317 (green).

<sup>1</sup> Edited by S. C. Jardin (jardin@pppl.gov)

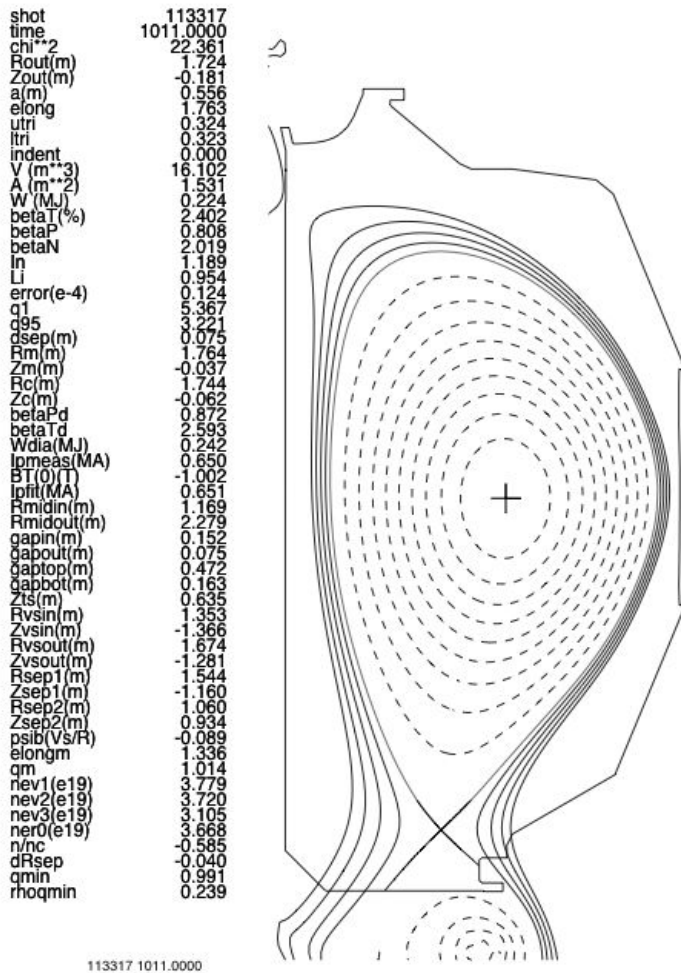


**Figure 2.** Poloidal cross section and parameters for shot 113317.

## 1.2 Linear and Non-linear Resistive MHD Studies

The linear stability and non-linear evolution of ELMs in these equilibria has been studied using the resistive MHD model in the NIMROD code. The time evolution of the kinetic energy in toroidal modes 1 through 43 is shown in Figures 3a and 3b. The linear growth rate as a function of toroidal mode number  $n$  for this case is shown in Figure 4. The primary linearly unstable modes are in the range  $5 < n < 25$ , with exact details depending on the equilibrium (see Figure 4). Other modes are driven non-linearly, some by two wave interaction and some by three wave interaction. The evolution of the temperature during the nonlinear evolution of an ELM in shot 113207 is shown in Figure 5, illustrating the formation of fingerlike structures near the plasma edge with increasingly fine structure as the calculation progresses.

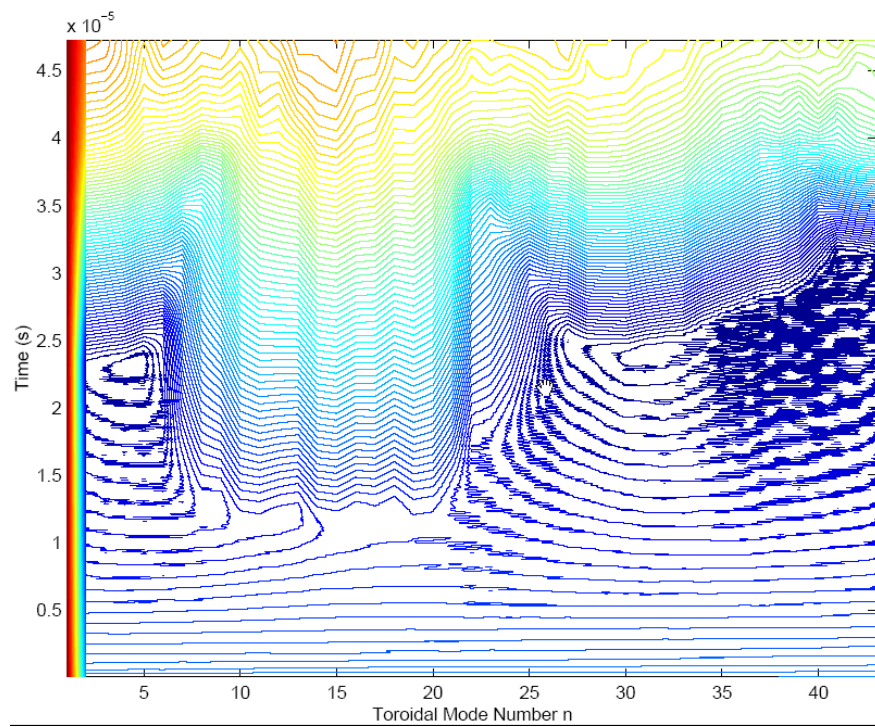


**Figure 3a.** Contour plot of kinetic energy in toroidal modes versus time for the non-linear evolution of shot 113207 using the resistive MHD model.

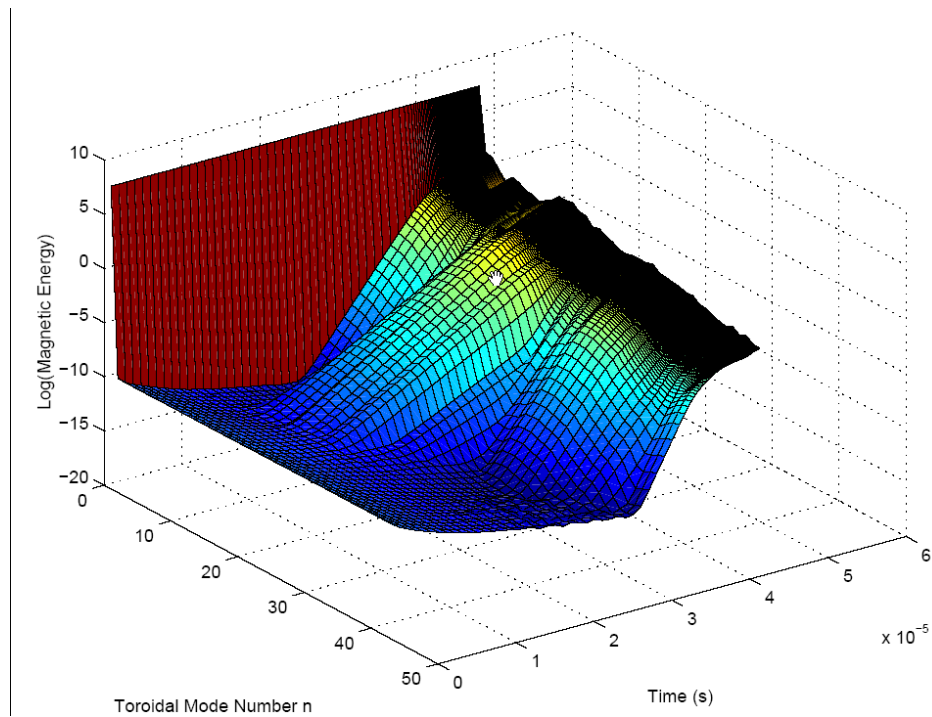


**Figure 3b.** Surface plot of kinetic energy in toroidal modes versus time for the non-linear evolution of shot 113207 using the resistive MHD model.

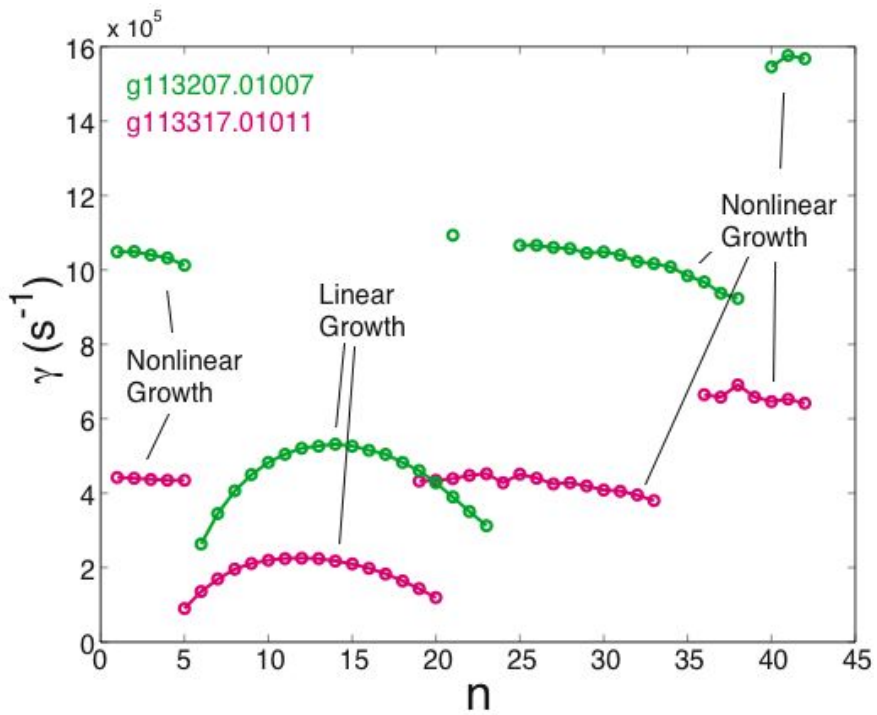


**Figure 4.** Growth rate versus toroidal mode number from the resistive MHD model for the two DIII-D equilibria under consideration. Linearly growing and non-linearly driven modes are identified.

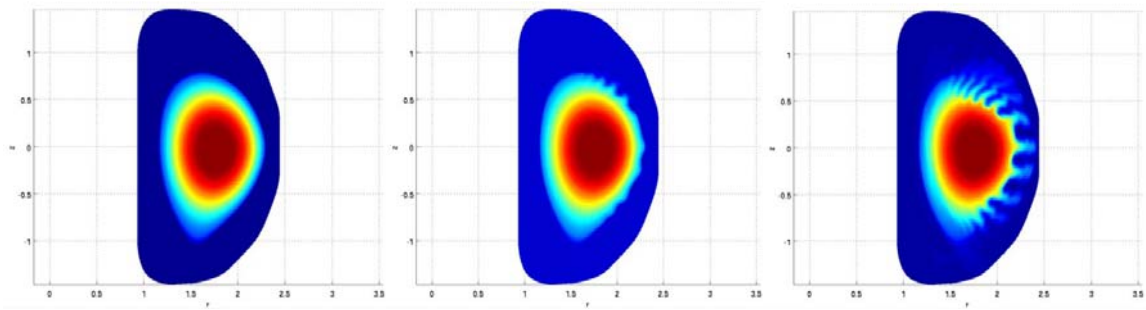


**Figure 5.** Evolution of the temperature during the non-linear evolution of an ELM in shot 113207.

### 1.3 Verification of the 2-fluid Model in NIMROD

In preparation for future nonlinear studies of the ELM, we are performing benchmark studies to gain confidence in the NIMROD 2-fluid model. In particular, the 2-fluid implementation in NIMROD has been validated against the ideal g-mode in a slab [K. V. Roberts and J. B. Taylor, Phys. Rev. Letters **8**, 197 (1962)]. Theory predicts two-fluid stabilization will occur when  $\omega_* > 2\gamma_{MHD}$ , where  $\omega_*$  is the drift frequency and  $\gamma_{MHD}$  is the MHD growth rate. Results from the NIMROD code are in excellent agreement with this prediction, as seen in Figure 6. Verification of the gyro-viscosity on this problem is underway.

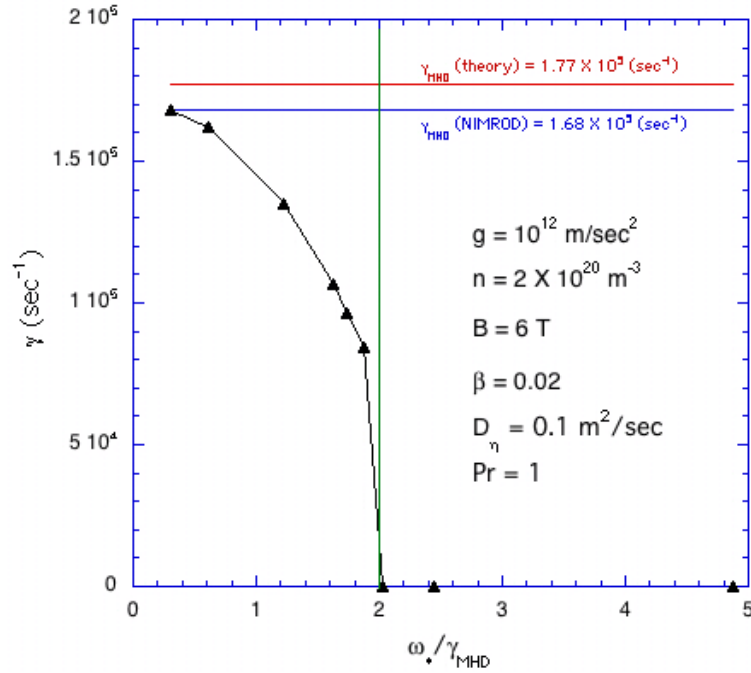


**Figure 6.** Growth rate of g-mode versus  $\omega_* / \gamma_{MHD}$  with 2-fluid effects in the NIMROD code.

## 1.4 Stability of Model Equilibria with Edge Density Gradients

Model equilibria with parameterized edge density gradients have been constructed. The density gradient can be shaped to match the equilibrium pressure profile according to  $n_{eq}(R, \theta) = (1 - \alpha_{nt})n_0 + \alpha_{nt}P_{eq}(R, \theta)/P_0$ . For the resistive MHD model, the growth rate has been determined for the  $n = 13$  mode with the NIMROD code as functions of the pedestal particle density (normalized to peak density), and the parameter  $\alpha_{nt}$ . The results are shown in Figures 7a,b.

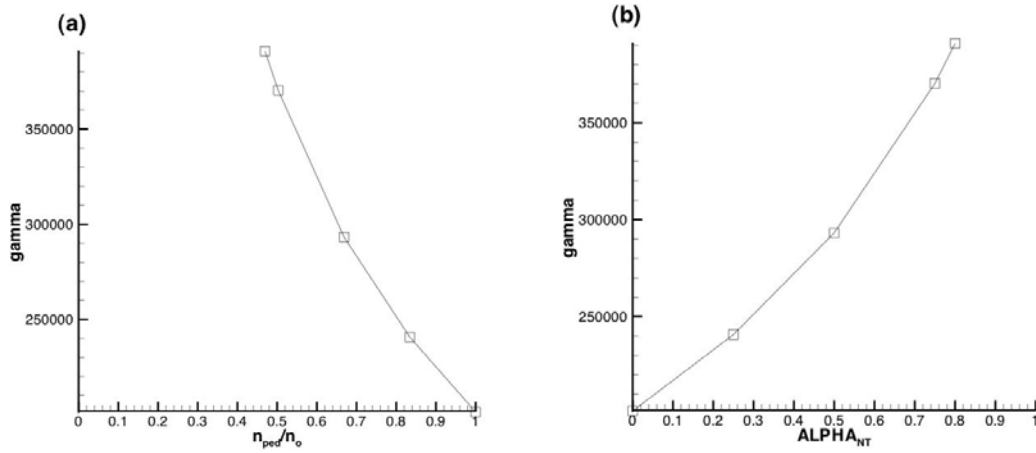


**Figure 7.** Linear growth rate for the  $n = 13$  mode in the resistive MHD model for the generic equilibrium **a)** versus normalized pedestal density, and **b)** versus pedestal height.

Linear stability calculations have also been run for these equilibria using the 2-fluid model in NIMROD. These are shown in Figure 8. Note that the linear growth rate actually increases compared with the resistive MHD case (see Figure 7.)

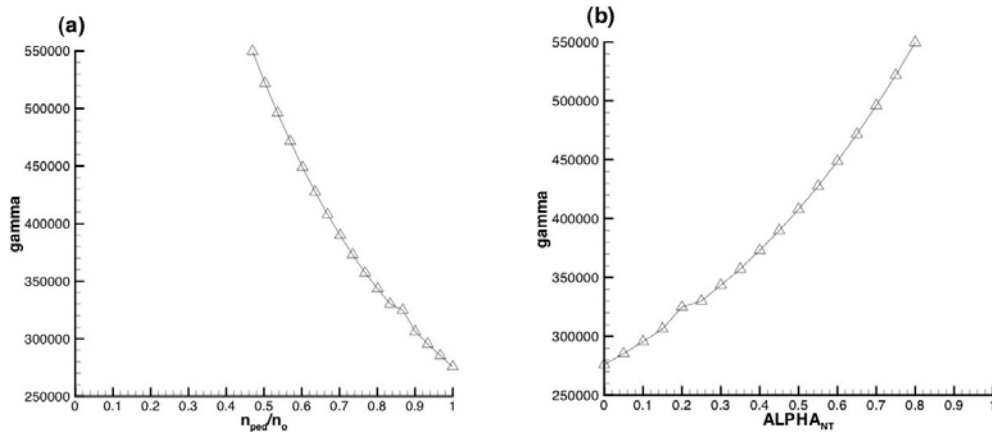


**Figure 8.** Linear growth rate for the  $n = 13$  mode in the 2-fluid MHD model for the generic equilibrium **a)** versus normalized pedestal density, and **b)** versus pedestal height. The growth rate has increased compared with the resistive MHD result (see Figure 7.)

## Section II: Studies with the M3D code

### 2.1 Density Dependence

In principle an ideal MHD instability growth rate should not be very affected by the edge pedestal. That is because the ideal MHD growth rate obtained from the energy principle is

$$\gamma^2 \int \rho \left| \vec{\xi} \right|^2 d^3x = \delta W \quad (1)$$

where  $\gamma$  is the growth rate,  $\rho$  is the mass density,  $\vec{\xi}$  is the displacement, and  $\delta W$  is the perturbed magnetic energy of the displacement. If the displacement  $\vec{\xi}$  vanishes in the “vacuum” outside the separatrix, then the value of  $\rho$  in the vacuum is irrelevant. If the displacement is nonzero but does not extend very far across the separatrix, then the value of  $\rho$  outside the separatrix should only make a small contribution.

A set of runs was performed starting from the EQDSK file *g113207.01007* (see Figure 1) which includes a density profile. The minimum density at the bottom of the pedestal is 0.18 times the peak density at the top of the pedestal. The density profile is shown in Figure 9. (NOTE: The density does not drop to zero at the right. This is just an artifact of the plot program).

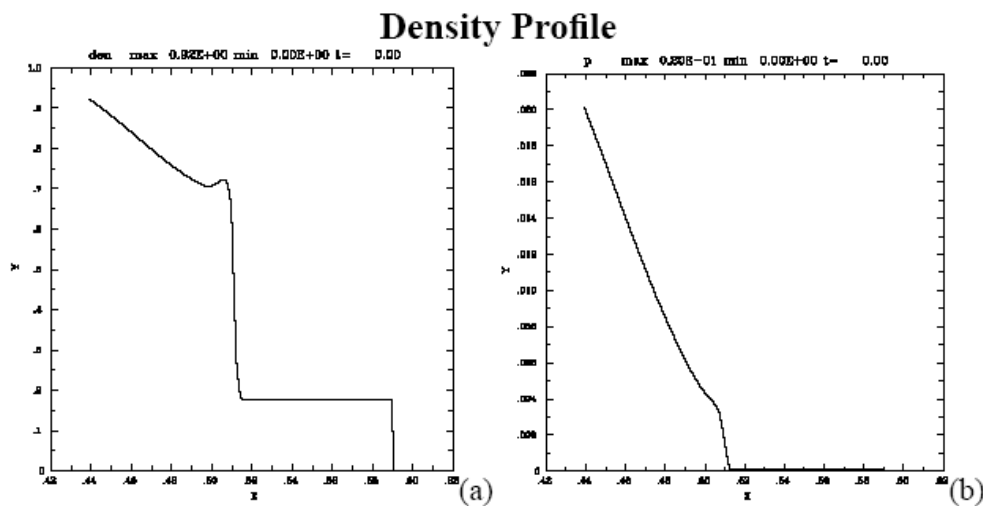


**Figure 9(a)** initial density profile along the major radius **(b)** initial pressure profile

The poloidal magnetic flux  $\psi$  is shown in Fig. 10. The initial equilibrium is shown in Fig 10(a), and the unstable mode perturbed flux is shown in Fig. 10(b), for density ratio 0.6.

## Magnetic Flux $\psi$ in DIII-D

a    max 0.15E-01  
min -0.70E-01 t= 67.15

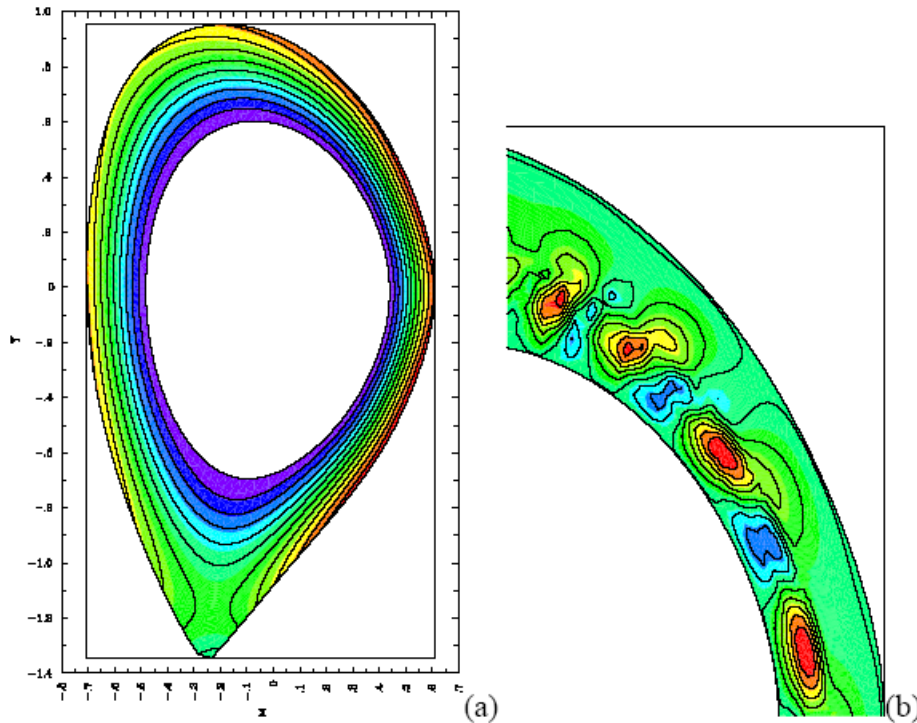


**Figure 10:** (a) initial poloidal magnetic flux (b) perturbed poloidal magnetic flux of unstable mode.

To assess the effect of the density gradient on the mode growth rate, a set of runs was done in which the density was a linear combination of the density profile in Fig. 9(a) and a constant density. Both profiles were normalized so that their peak values were unity. The minimum value of the density was then varied by taking different linear combinations of the profiles. The results are shown in Fig. 11.

The growth rate is plotted as a function of the relative density at the bottom of the pedestal. The growth rate is seen to be independent of the relative density, as long as the density ratio is greater than about 0.3. However, when the ratio was less than this, the growth rate became much larger. We have verified that the reason for this was not because the time step was too large. However, further research is needed to identify the cause of this behavior, in particular to determine if it is physical or a numerical artifact.

It is anticipated that simulations with sufficiently high resolution should give reasonable results. In any event, it is clear that the nonlinear evolution of ELMs in equilibrium with a steep pedestal density gradient is a challenging problem.

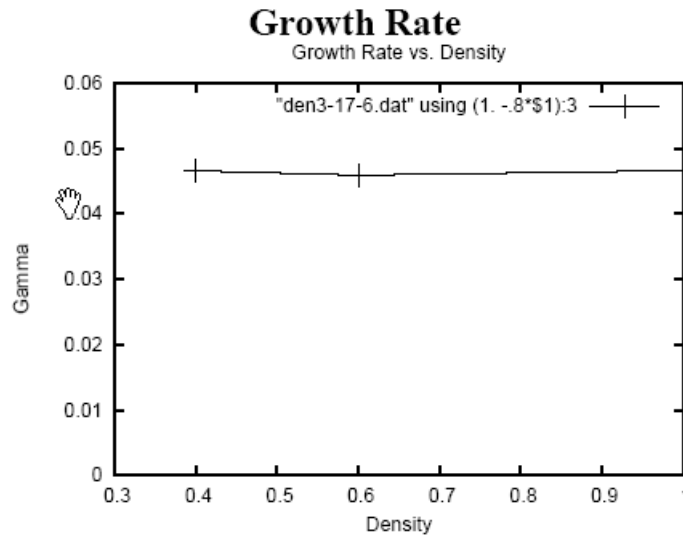


**Figure 11:** Growth rate as a function of relative density at the bottom of the pedestal. The minimum possible value is  $0.18$ .

## 2.2 Improving the representation of the Boundary

The other topic of the milestone is improving representation of the outer boundary. This is being done in M3D by patching together meshes generated in two ways. The inner mesh is a regular mesh aligned with the poloidal magnetic flux  $\psi$  inside the separatrix, and expanded outward across the separatrix, close to the wall. Between this mesh and the wall is a second mesh, generated with the Triangle code, which is not aligned with flux surfaces. An example mesh for ITER, using the EQDSK file *iter\_Ped\_ref\_129\_gfile*, is shown in Fig. 12(a). The outer boundary is the ITER first wall. The magnetic flux function is shown in Fig. 12(b). A closeup of the outboard portion of the mesh is displayed in Fig 13(a). Contours of pressure during a nonlinear ELM simulation are shown in Fig. 13(b).

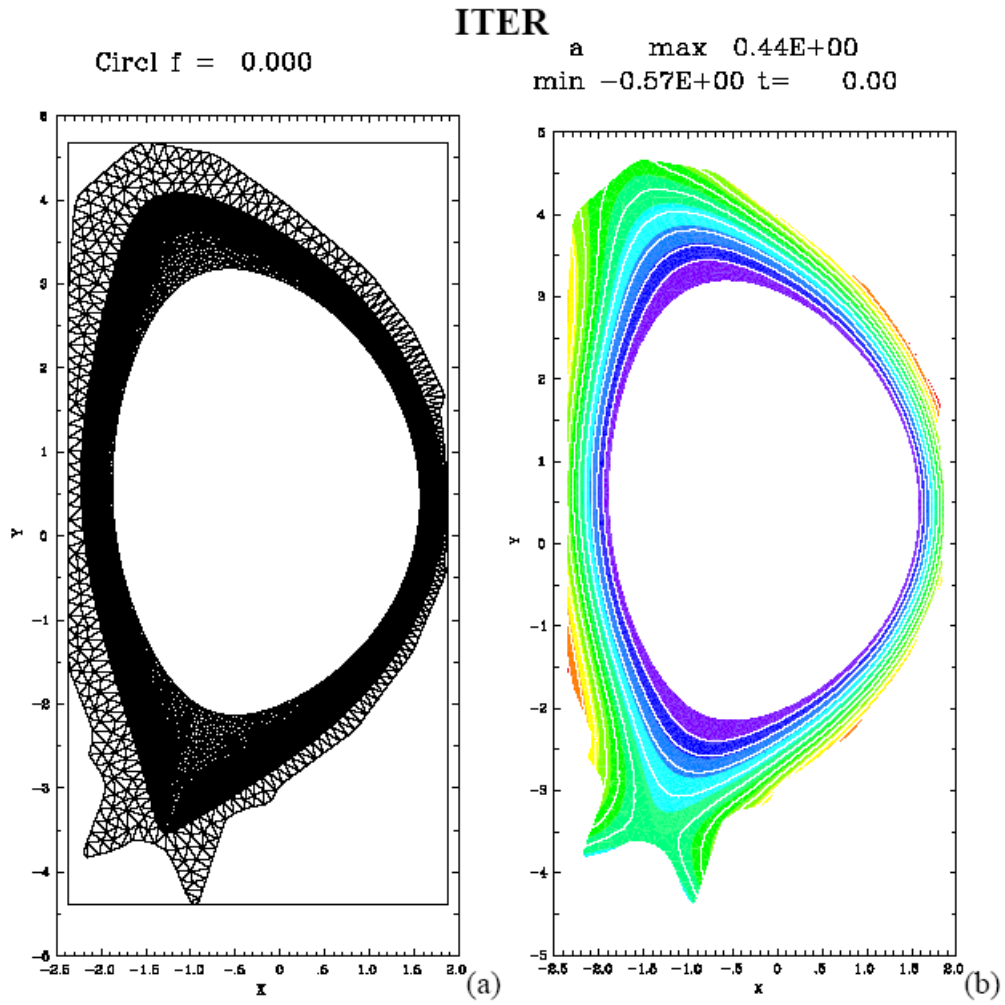


**Figure 12:** (a) ITER mesh, (b) ITER magnetic flux function

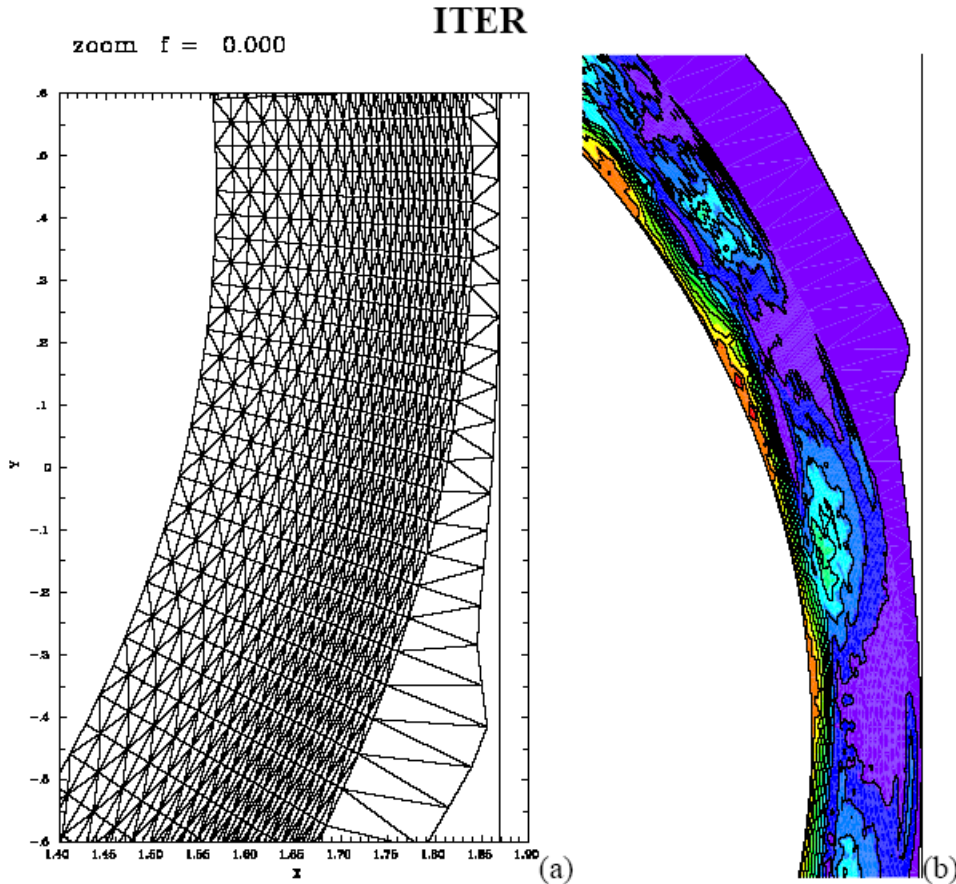


**Figure 13: (a) ITER Mesh (b) pressure during an ELM**

### Section III. Summary

The Q2 ELM milestones have been successfully completed with contributions utilizing both the NIMROD and M3D codes. Two representative DIII-D equilibria with steep edge density gradients have been chosen for further study. Initial nonlinear resistive MHD simulations of these equilibria have been performed keeping over 40 toroidal modes. The nonlinear evolution drives higher modes and leads to highly localized structure. The NIMROD effort is now beginning to incorporate 2-fluid effects into their model which should have the effect of suppressing the short-wavelength (high  $n$ ) modes. However, the linear growth rate of moderate- $n$  modes actually increases with the 2-fluid model in NIMROD. (See the Q1 milestone report for a companion study with the M3D code).

The M3D code has made several modifications to enable it to better deal with the steep edge density gradients and to better represent realistic geometry. Unexpected behavior can still occur for extreme values of the density gradients, and this is being further studied. A new meshing technique has been implemented in M3D to allow more accurate representation of the plasma/vacuum and vacuum vessel boundaries.